ผลของกลยุทธ์การประจุไฟสำหรับแบตเตอรี่สังกะสีอากาศ

นายวัชระพิศุทธ ธนพงศ์อมร



วิทยานิพนธ์นี้เป็นส่วนหนึ่งของการศึกษาตามหลักสูตรปริญญาวิศวกรรมศาสตรมหาบัณฑิต
สาขาวิชาวิศวกรรมเคมี ภาควิชาวิศวกรรมเคมี
คณะวิศวกรรมศาสตร์ จุฬาลงกรณ์มหาวิทยาลัย
ปีการศึกษา 2558

# Effects of recharging strategy for zinc-air battery

Mr. Wacharapisuth Thanapong-a-morn


A Thesis Submitted in Partial Fulfillment of the Requirements
for the Degree of Master of Engineering Program in Chemical Engineering
Department of Chemical Engineering
Faculty of Engineering
Chulalongkorn University
Academic Year 2015

| | |
|---|---|
| Thesis Title | Effects of recharging strategy for zinc-air battery |
| By | Mr. Wacharapisuth Thanapong-a-morn |
| Field of Study | Chemical Engineering |
| Thesis Advisor | Associate Professor Dr.Soorathep Kheawhom, Ph.D. |

Accepted by the Faculty of Engineering, Chulalongkorn University in Partial Fulfillment of the Requirements for the Master's Degree

.....Dean of the Faculty of Engineering
(Associate Professor Dr.Supot Teachavorasinskun, D.Eng.)

THESIS COMMITTEE

.....Chairman
(Dr. Pimporn Ponpesh, Ph.D.)

.....Thesis Advisor
(Associate Professor Dr.Soorathep Kheawhom, Ph.D.)

.....Examiner
(Assistant Professor Dr. Amornchai Arpornwichanop, D.Eng.)

.....External Examiner
(Dr.Pornchai Bumroongsri, D.Eng.)

วัชระพิศุทธ ธนพงศ์อมร : ผลของกลยุทธ์การประจุไฟสำหรับแบตเตอร์รี่สังกะสีอากาศ (Effects of recharging strategy for zinc-air battery) อ.ที่ปรึกษาวิทยานิพนธ์หลัก: รศ. ดร. สุรเทพ เขียวหอม, 52 หน้า.

งานวิจัยนี้นำเสนอกลยุทธ์การประจุไฟสำหรับแบตเตอร์รีสังกะสี-อากาศเพื่อที่จะศึกษาสมรรถภาพในการประจุไฟซึ่งรวมถึงเวลาในการประจุไฟ ประสิทธิภาพในการประจุไฟ และความเสถียรในแต่ละวัฏจักรของแบตเตอร์รีโดยพิจารณาผลกระทบที่เกิดจากปฏิกิริยาการเกิดออกซิเจนและปฏิกิริยาการแตกตัวของน้ำด้วยไฟฟ้าข้างเคียงซึ่งเป็นปฏิกิริยาข้างเคียง โดยผลกระทบของปริมาณของความหนาแน่นกระแสที่มีต่อการเกิดออกซิเจนและปฏิกิริยาข้างเคียงจะถูกศึกษา นอกจากนี้กลยุทธ์การประจุไฟแบบต่างๆถูกคิดค้นขึ้นเพื่อปรับปรุงสมรรถภาพในการประจุไฟของแบตเตอร์รี่ ผลการทดลองเป็นผลจากการจำลองโดยใช้โปรแกรมแมทแลป พบว่าการประจุไฟด้วยความหนาแน่ความแสปริมาณสูงเป็นผลให้การประจุไฟล้มเหลวได้เนื่องจากฟองออกซิเจนที่เกิดขึ้นจากอัตราการเกิดออกซิเจนสูง ปัญหานี้ถูกจัดการได้โดยการใช้กลยุทธ์การประจุไฟแบบสองชั้นและหลายชั้นซึ่งเป็นผลให้สามารถประจุไฟได้ 100% ของสถานะของประจุโดยมีประสิทธิภาพมากในเวลาอันสั้นและยังให้ความเสถียรในแต่ละวัฏจักรของแบตเตอร์รีอีกด้วย สำหรับปฏิกิริยาข้างเคียงพบว่าไม่มีผลกระทบโดยเฉพาะต่อแบตเตอร์รีขนาดเล็ก



ภาควิชา วิศวกรรมเคมี ลายมือชื่อนิสิต .....

สาขาวิชา วิศวกรรมเคมี ลายมือชื่อ อ.ที่ปรึกษาหลัก .....

ปีการศึกษา 2558

# # 5770297621 : MAJOR CHEMICAL ENGINEERING
KEYWORDS: ZINC-AIR BATTERY / RECHARGING STRATEY / OXYGEN EVOLUTION REACTION / SIDE REACTION

WACHARAPISUTH THANAPONG-A-MORN: Effects of recharging strategy for zinc-air battery. ADVISOR: ASSOC. PROF. DR.SOORATHEP KHEAWHOM, Ph.D., 52 pp.

This research presents recharging strategies for zinc-air battery to study its recharging performance including recharging time, efficiency and cycling stability resulted from oxygen evolution reaction and water electrolysis reaction which is side reaction. The effects of recharging current density on these reactions are studied. In addition, various recharging strategies are also investigated to improve recharging performances of the battery. The results are obtained through simulation in Matlab. It was found that recharging with high current density resulted in incomplete of recharging process due to oxygen bubbles growth from high rate of oxygen evolution. This problem can be overcome by two-stage and multi-stage recharging strategies which yield 100% state of charge (SOC) of the battery with high efficiency in short time. Furthermore, the cycling stability of the battery is improved by these strategies. As for the effects of side reaction, it affects insignificantly small scale battery.



Department: Chemical Engineering Student's Signature .....
Field of Study: Chemical Engineering Advisor's Signature .....
Academic Year: 2015

# ACKNOWLEDGEMENTS

Firstly, I would like to thanks my advisor, Associate Professor Dr.Soorathep Kheawhom, who always suggests and helps me in both thesis and education. Furthermore, this thesis will not be able to complete absolutely unless there is his guidance.

In addition, I also would like to thank my thesis committee members, Dr.Pimporn Ponpesh, Assistant Professor Dr.Amornchai Arpornwichanop and Dr.Pornchai Bumroongsri for their useful comments and their time on my thesis. I then like to thank my friends at Computational Process Engineering Research Center for giving me various suggestions and helps.

Finally, I would like to express my sincere gratitude to my parents. Unless my parents support me, I will not have an opportunity to graduate my master's degree.

**CONTENTS**

Page

Page

# LIST OF TABLES

Page

# LIST OF FIGURES

Page

# Chapter I
# Introduction

## 1.1 Importance and reasons

Electricity can be produced from a variety of renewable energy sources. Among them, solar photovoltaic (PV) technology is widely utilized because of its low cost and simplicity. PV generate direct current electricity from solar radiation without contribution to environmental impact. Nevertheless, the electricity produced from PV is uncertain because of the intermittent nature of solar radiation. Moreover, high dependency on weather condition and season are the main limitation of PV. Therefore, batteries are usually employed with PV system.

Metal-air batteries are becoming of particular interest for their high specific energy density (Xu, Ivey et al. 2015). Among them, zinc-air batteries are the most promising solution for energy storage application. Because of their relatively high theoretical energy density, low toxicity and environmentally friendly. Moreover, zinc are the most electropositive metal that is relatively stable in aqueous and alkaline media without significant corrosion (Li and Dai 2014).

The zinc-air batteries work on the basis of reaction between the atmospheric oxygen and zinc pellet in liquid alkaline electrolyte. In discharging process, zinc is converted to zinc oxide by reacting with hydroxide ions produced from oxygen reduction reaction (ORR). Electrons are discharged from zinc electrode and transferred to air electrode across the external load. On the other hand, in recharging process, hydroxide ions are reduced by oxygen evolution reaction (OER) at air electrode.

Electrons are consumed and transferred back to zinc anode. After that, zinc oxide accepts the electrons and electrochemically converts to zinc metal.

During recharging process, zinc-air batteries involve oxygen evolution reaction (OER). Coalescence of generated oxygen bubbles occurs at the air electrode of zinc-air batteries during the recharging process (Wang, Pei et al. 2015). The oxygen bubbles easily adhere to the surface of air electrode surface and reach a critical value resulting in increasing of ohmic resistance. The oxygen bubbles also reduce recharging efficiency and damage the batteries.

In addition to problems with oxygen, another one that can occur during recharging process of the battery is side reaction. $H_2O$ is only electrochemically stable below -0.82 V vs. SHE (standard hydrogen potential). This can lead to unwanted side reaction, the hydrogen evolution reaction (HER). This reaction has two negative effects on Zinc-air batteries during recharging process. It consumes the water which is used to produce active material $Zn$ , and forms hydrogen gas, which will expand the sealed zinc electrode and might cause structure change for the entire battery, or even complete battery failure. To handle the problem on oxygen bubbles generated, suitable recharging strategy is necessary.

Several recharging strategies have been investigated. Using constant current density is a traditional simple recharging strategy which is widely used. Multi-step constant current densities is another strategy which can prolong battery life, shorten recharging time and increase recharging efficiency (Ikeya, Sawada et al. 1998, Ikeya, Sawada et al. 2002).

Mathematical model of zinc-air battery has been developed to study behavior of rechargeable zinc-air battery during discharging and recharging process (Deiss, Holzer et al. 2002). During discharging process, the effects of the impact of surrounding air composition on discharging performance of the battery are analyzed by using the model (Daniel Schröder and Ulrike Krewer 2014). Moreover, the effects of oxygen evolution reaction during recharging process are also studied by oxygen bubbles growth model (Wang, Pei et al. 2015). It is noted that the generated oxygen has limited the recharging performance. Therefore, the recharging strategy must be investigated by using zinc-air battery model because of its experimental study is very time-consuming.

In this work, mathematical model of zinc-air battery is developed in Matlab. The model is used to study an effect of recharging current on oxygen bubbles growth. Then, the recharging strategy is investigated to complete recharging process with shorten recharging time and high recharging efficiency. Moreover, cycling stability of the battery is also investigated

## 1.2 Objectives

1) To develop rechargeable zinc-air battery model including oxygen bubble model and side reaction model
2) To study the effect of current density on oxygen evolution rate and side reaction occurred during recharging process.
3) To investigate recharging strategy of zinc-air battery

## 1.3 Scopes of work

1) Simulation of zinc-air battery is performed by Matlab software.
2) Parameters used in this work are obtained from published experimental results.
3) Polarization curve of zinc-air battery is validated with published experimental results.
4) Effect of current density on oxygen growth rate is studied during recharging process of zinc-air battery.
5) Effect of current density on side reaction is studied during recharging process of zinc-air battery.
6) Two-stage and multi-stage constant recharging current density are studied.

## 1.4 Organization of thesis

Chapter II reviews overviews of zinc-air battery model and problem in recharging process include oxygen bubble growth and side reaction. In addition, recharging technics are also review in this chapter.

Chapter III presents regarding principle of zinc-air battery along with its mathematical model, the oxygen bubble model and side reaction model. Besides, calculation of state of charge and recharge efficiency of the battery are presented as well.

Chapter IV describes the simulation procedure and validation of the simulated results used in this work and also defines parameters and initial value of presented results.

Chapter V introduces the results concerning effect of recharging current density on oxygen evolution rate and effects of side reaction on recharge process of zinc-air battery. Moreover, recharging strategies are proposed and analyzed properly.

Chapter VI gives conclusion and recommendation with respect to the use of mathematical models of the zinc-air battery as well as recharging strategies.

# Chapter II
# Literature reviews

Literature reviews on recharging strategy of zinc-air battery are presented in this chapter. The reviews include four sections; Zinc-air battery modeling, oxygen evolution during recharging process, water electrolysis side reaction and recharging technique. The first section introduces the model of zinc-air battery which used to predict performance of the battery. The zinc-air battery involve oxygen evolution reaction during recharging process then in section 2, the bubble growth model is studied. The occurred oxygen bubbles may cause of stop recharging. Another section, side reaction during recharging process of zinc-air battery which is cause of significant decrease in cycle life of battery is mentioned. To solve both oxygen bubble and side reaction problem, the recharging strategy is investigated.

## 2.1 Zinc-air battery modeling



According to research on zinc-air battery is almost experimental and focuses on material characterization that is very time-consuming, hence, mathematical models can be helpful to analyze performance and lifetime of zinc-air battery.

A one-dimensional numerical model of zinc-air battery was developed by Deiss, Holzer et al. (2002) to analyze the experimental data. They found that the model was used to extend calculations of three cycles of experiment up to 40 cycles. They also noted that agreement between model calculation and experiment are attained.

Moreover, the basic mathematical models of rechargeable zinc-air battery was presented by Daniel Schröder and Ulrike Krewer (2014) to investigate impact of

surrounding air on zinc-battery. They found that limiting of zinc-air battery operation increases with concentration of surrounding oxygen. The presented model approach and the achieved result might be used to investigate other metal air battery with liquid electrolyte.

## 2.2 Oxygen evolution reaction

The related problem at the air cathode is sluggish oxygen reactions. They are cause of power density limited and recharging problem due to high over-potential is required for ORR and OER. For OER, the phenomena of bubbles will arise when the oxygen concentration in the electrolyte gets saturated. Oxygen bubbles can move along electrode surface, leading to bubbles coalescence. The effects of oxygen bubbles coalescence on recharging zinc-air battery performance were studied by Wang, Pei et al. (2015). They found that oxygen bubbles coalescence can prevent the contact between electrolyte and electrode result in failure of the recharging. Furthermore, they suggested the two solution for improve recharging the battery that are Partial insulation of recharging electrode and hydrodynamic electrolyte.

## 2.3 Water electrolysis

Water is only electrochemically stable below -0.82 V vs. SHE (standard hydrogen potential). This can lead to unwanted side reaction, the hydrogen evolution reaction (HER) of water electrolysis, in zinc air battery during recharging process. Various technologies are available to hydrogen production by water electrolysis. The most common is alkaline electrolysis, proton exchange membrane (PEM), and solid oxides. The concept is two electrodes and an electrolyte that allows the transport of

ions. The alkaline water electrolysis process usually operates with electrolyte concentrated with KOH and its operating temperature is between 60 to 90 °C. This process has two types of losses that are ohmic overpotential and activation overpotential. Hydrogen and oxygen bubble which are produced at the cathode and anode, respectively is a one cause of ohmic overpotential. As for the behavior of bubbles in KOH solution, it was characterized by Janssen, Sillen et al. (1984). The bubbles parameter such as radius, volume and density were determined based on experimental data in dependence on current density, pressure, temperature and concentration of KOH.

## 2.4 Recharging techniques

From section 2, the generated oxygen bubbles coalescence during recharging zinc-air battery are cause of recharging problem. Therefore, suitable recharging strategy should be investigated. Several recharging techniques which use to recharge batteries are reviewed in this section.



The most widely-used traditional recharging technique is constant current constant voltage (CCCV). This technique is divided into two stages, first stage starts with constant current recharging until a terminal voltage is reached, and then followed by the second stage. A constant voltage is used to recharge battery until predefined current is reached. The CCCV technique allows an almost full battery capacity but it increases charging time compared to constant current (CC). A comparison of different techniques of recharging is presented by Cope and Podrazhansky (1999). It was found that recharging by using low constant current is low economical but does not optimize the battery performance. The multi-stage constant current technique is investigated as optimal recharging technique by Ikeya, Sawada et al. (1998) and, in addition, the two-

stage constant current technique was compared with multi-stage constant current. They found that the multi-stage constant current technique allow complete recharging battery with much shorter time and higher recharging efficiency than two-step constant current technique.

Recently, battery recharging process is considered as an optimizing problem with cost function of recharging time and energy loss. The optimal control theory is used to solve this problem by Abdollahi, Han et al. (2016). In addition, the current profile is investigated to minimize the cost function weighted sum of recharging time and energy loss. They presented the well-known technique CCCV is the optimal technique in that case. The profile of recharging current in CC stage is function of ratio of weighting on recharge time and energy loss.

# Chapter III
# Theory

## 3.1 Principle of zinc-air battery

A zinc-air battery is an electrochemical device which produces electrical energy from chemical energy. A basic structure of the battery consists of electrolyte layer sandwiched between two electrodes. The anode material is zinc which possesses high specific energy density and low toxicity. Moreover, it is the most electropositive metal that is relatively stable in aqueous and alkaline media without significant corrosion (Li and Dai 2014). The air cathode is composed of a hydrophobic membrane, a catalytic layer and a current collector. The structure of zinc-air battery is shown in Figure. 3.1. At the anode, where the oxidation of zinc take place, zinc convert to zinc oxide by reacting with hydroxide ions. During the conversion, electrons are discharge and transferred to the anodic current collector. The electrons on the anode pass across the external load and come back to the cathode current collector. At the cathode, where the reduction of oxygen take place, air or any oxygen source is electrochemically reduced to hydroxide ions by reacting with water on the surface of gas-permeable membrane when it is supplied. The overall electrochemical reaction taking place in the zinc-air battery can be analyzed by considering the anode and the cathode reactions as express in equations (3.1) and (3.2). The overall reaction can be expressed as equation (3.3).

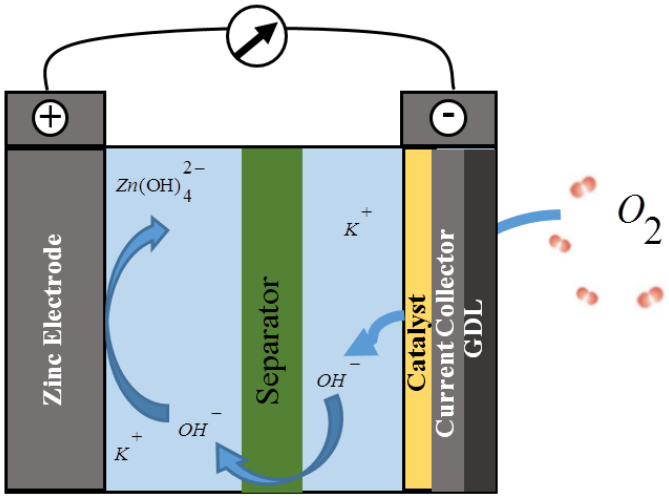


**Figure 3.1** Schematic of zinc-air battery.

Anode: $Zn + 4OH^- \rightleftharpoons Zn(OH)_4^{2-} + 2e^-$ (3.1)

$Zn(OH)_4^{2-} \rightleftharpoons ZnO + H_2O + 2OH^-$

Cathode: $O_2 + 4e^- + 2H_2O \rightleftharpoons 4OH^-$ (3.2)

Overall reaction: $2Zn + O_2 \rightleftharpoons 2ZnO$ (3.3)

The standard potential of zinc-air battery is 1.65 V. In practice, its working voltage is obviously lower than 1.2 V in order to get various discharge current densities (Li and Dai 2014).

In most case of battery type, the performance is usually expressed in term of polarization curve as shown in Figure. 3.2. Polarization represent the voltage change in term of the current density change. It can be divided to three zone as activation loss, ohmic loss and concentration loss. The slowness of reactions taking place on the surface

of the electrodes result in activation loss zone. This zone ranging from open circuit voltage at zero current density to the steep of voltage decrease. The ohmic loss zone, where the voltage slowly drop, occurs due to electrical resistance of electrodes and interconnections. Moreover, the resistance to flow of ions in electrolyte is also cause of ohmic loss zone. For the last zone, the voltage rapidly fall at high current density because of mass transport effect.

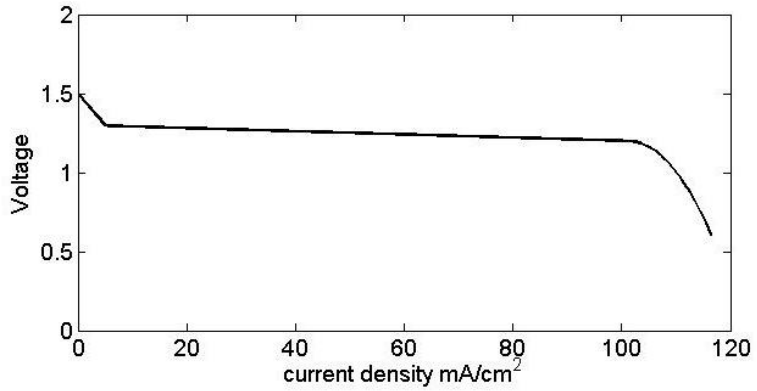


**Figure 3.2** polarization curve (Sapkota and Kim 2009).

For rechargeable zinc-air battery, electrochemical reaction can revert when 2.0 volt of recharging voltage or higher is applied. In addition, air electrode should be capable of catalyzing both oxygen reduction reaction during discharge and oxygen evolution reaction during recharge. This can be achieved by using bifunctional oxygen catalyst such as $Co_3O_4$. Recently, there are several bifunctional catalysts that have been researched but degradation usually starts within few numbers of cycles. Therefore, highly efficient and robust bifunctional electrocatalyst for rechargeable zinc-air battery. However, water electrolysis can occur during recharging process due to low standard hydrogen potential of hydrogen evolution reaction which is expressed below:

$$4H_2O + 4e^- \rightleftharpoons 2H_2 + 4OH^- \quad (3.4)$$

This reaction is able to react with oxygen evolution reaction (equation (3.2)) which requires the standard potential only 1.23 V to split the water. Water electrolysis has two negative effects on Zinc-air batteries during recharging process. It consumes the water which is used to produce active material $Zn$, and forms hydrogen gas, which will expand the sealed zinc electrode and might cause structure change for the entire battery, or even complete battery failure

### 3.2 Zinc-air battery model

In this section, the general equations that are used in this work are presented. In addition, the basic principle of electrochemical is proposed with many assumptions as follow:

1) No concentration gradients along all electrode dimension.
2) Dilute solution behavior.
3) Isothermal operation at temperature is 298.15 K.
4) Constant active electrode areas and zinc electrode thickness.
5) A change of liquid electrolyte volume in gas diffusion layer at the air electrode does not significantly increase the amount of water in the pores.
6) Dissolved oxygen are not able to pass through the separator.

Nernst potential equation which relates to reduction potential of half-cell potential is used to calculated cell potential of the battery. In addition, mass

conservation Nernst-Planck equation is used to describe motion of chemical charged species in fluid medium. The molar flow rates exchange of ions under the influence of both concentration gradient and electric field are also calculated.

The cell potential of zinc-air battery consist of the open circuit potential the over-potentials at zinc and air electrode. It is expressed in equation (3.4):

$$E^{cell} = E^{0,cell} - \eta^{zinc} - \eta^{air} \tag{3.4}$$

where $E^{0,cell}$ is a standard cell potential which is given by the Nernst potential, $\eta^{zinc}$ and $\eta^{air}$ are over-potentials of zinc and air electrode, respectively. As for ohmic over-potential, it is neglected due to this loss is very small. The standard cell potential ($E^{0,cell}$) and potentials for electrodes ($E^{0,air}$, $E^{0,zinc}$) are represented in equation (3.5) - (3.7) (Daniel Schröder and Ulrike Krewer 2014):



$$E^{0,cell} = E^{0,air} - E^{0,zinc} \tag{3.5}$$

$$E^{0,air} = 0.401 + \frac{RT}{zF}\ln\left(\frac{[\mathrm{Ox}]}{[\mathrm{Red}]}\right) \tag{3.6}$$

$$E^{0,\mathrm{zinc}} = -1.266 + \frac{RT}{zF}\ln\left(\frac{[\mathrm{Ox}]}{[\mathrm{Red}]}\right) \tag{3.7}$$

For redox reactio $Ox + ne^- \rightarrow Red$ n where $Ox$ is oxidized state, $Red$ is reduced state, $R$ is gas constant (J/Kmol), $T$ is temperature (K), $z$ is number of participated electrons in reaction, $F$ is Faraday constant (C/mol).

The reaction rate of equation (3.1) and (3.3) at the zinc and air electrode are described with a Butler-Volmer approach. Both reaction rates are expressed in equation (3.8) and (3.9) (Deiss, Holzer et al. 2002). As for reaction rate of equation (3.2), the saturated approach is accounted as $r_2$.

$$r_1 = -\left[k_1^{Ox}[Ox]\exp\left(\frac{-(1-\alpha^{Ox,zinc})F}{RT}\eta^{zinc}\right) - k_1^{Red}[Red]\exp\left(\frac{(\alpha^{Red,zinc})F}{RT}\eta^{zinc}\right)\right] \tag{3.8}$$

$$r_3 = \left[k_3^{Ox}[Ox]\exp\left(\frac{-(1-\alpha^{Ox,air})F}{RT}\eta^{air}\right) - k_3^{Red}[Red]\exp\left(\frac{(\alpha^{Red,air})F}{RT}\eta^{air}\right)\right] \tag{3.9}$$

where $k_i^n$ is rate constant for reaction i = 1,3 and reaction state n = oxidized state and reduced stated, $\alpha$ is charge transfer coefficient.

The mass balance equation in zinc-air battery base on molar concentration in liquid electrolyte can be calculated as follow (Daniel Schröder and Ulrike Krewer 2014):

$$\frac{dc_k^j}{dt} = J_k^{j,diff} + J_k^{j,mig} + J_k^{j,conv} + \frac{\sum \nu_{k,i} \cdot r_i}{V_{electrolyte}^j} - \frac{c_k^j}{V^j} \cdot \frac{dV_{electrolyte}^j}{dt} \tag{3.10}$$

where $c_k^j$ is molar concentration of species $k = ZnO, OH^- ZnOH_4^{2-}$ within electrode j, $v_{k,i}$ is stoichiometric coefficient of species k in reaction i, J is molar flow rate exchange between both electrode

The molar flow rates of exchange for species k including diffusion (diff), migration (mig) and convection (conv) molar flow rate are described with Nernst-Planck equation as follow equations:

$$J_k^{j,diff} = D_k \frac{(c_k^{air} - c_k^{zinc})}{\delta^{sep}} \varepsilon^{sep} A^{sep} \tag{3.11}$$

$$J_k^{j,\mathrm{mig}} = \frac{t_k}{z_k F} i^{cell} \varepsilon^{sep} A^{sep} \tag{3.12}$$

$$J_k^{j,\mathrm{conv}} = F^{conv} c_k^{zinc} \tag{3.13}$$

Volume electrolyte at zinc and air electrode is changing with time during discharge and recharge. At zinc electrode, the total volume of electrode is not change with time but solid volume of zinc particle change, thus the volume change of electrolyte at zinc electrode can be written as shown in equation (3.14) (Deiss, Holzer et al. 2002). As for air electrode, only volume of electrolyte is changing with time.

$$\frac{dV_{electrode}^{zinc}}{dt} = \frac{dV_{solid}^{zinc}}{dt} + \frac{dV_{electrolyte}^{zinc}}{dt} = 0 \tag{3.14}$$

$$V_{solid}^{zinc} = n_{Zn} \cdot \tilde{V}_{Zn} + n_{ZnO} \cdot \tilde{V}_{ZnO} \tag{3.15}$$

$$\frac{dV_{electrolyte}^{air}}{dt} = -F^{conv} + r_3 \sum_m v_{m,3} \tilde{V}_m + \sum_g J_g^{air,diff} \tilde{V}_g + \sum_g J_g^{air,\mathrm{conv}} \tilde{V}_g + \sum_h J_h^{air,\mathrm{mig}} \tilde{V}_h$$

(3.16)

where $V_{solid}^{zinc}$ is solid volume of zinc particle which is defined by partial molar volume $\tilde{V}$ of the respective species, $V_{electrolyte}^{zinc}$ is volume of electrolyte at zinc electrode, $V_{electrolyte}^{air}$ is volume of electrolyte at air electrode, $m = OH^-, H_2O$ , $g = OH^-, \mathrm{K}^+, ZnOH_4^{2-}, H_2O$ , $h = OH^-, ZnOH_4^{2-}, H_2O$ , $F^{conv}$ is convective flow defined as coming from zinc electrode with negative sign.

### 3.3 Oxygen model

Oxygen bubble evolution is depend on concentration gradient of oxygen between gas phase and liquid phase, leading to the bubble growth. There are many equations which represent the behavior of oxygen bubble growth but here the equation of Rayleigh-Plesset was applied to study the bubble growth in electric field. As for the bubble growth rates due to mass diffusion are so slow, the convective term of diffusion equation is negligible then the the equation which represent model of oxygen bubble evolution can be set up as follow:

$$R\frac{dR}{dt} = \frac{D\{\mathrm{c}_\infty - \mathrm{c}_s(1+2S/Rp_\infty)\}}{\rho_G(1+4\mathrm{S}/3\mathrm{Rp}_\infty)}\{1+\mathrm{R}(\pi\,\mathrm{Dt})^{-\frac{1}{2}}\} \qquad (3.16)$$

where $R$ is the radius of bubble in a liquid at a fixed ambient pressure , $p_\infty$, and uniform gas concentration, $c_\infty$. D is diffusivity of oxygen in electrolyte and $c_s$ is concentration of gas at liquid interface which is equal to partial pressure of gas in bubble divided by Henry's constant. The last term of this equation arises from a growing diffusion boundary layer in the liquid at the bubble surface. Once t is large, this term becomes small. For simplicity the surface tension is neglected. Then the characteristics growth is given by

$$R(\mathrm{t})^2 - R(0)^2 \approx \frac{2D(\mathrm{c}_\infty - \mathrm{c}_s)\mathrm{t}}{\rho_G} \tag{3.17}$$

Parameters of bubble are obtained from experimental data, which are published by Janssen, Sillen et al. (1984), when radius of bubble in equation (3.17) is calculated. In addition, radius of bubbles are equivalent is assumed and circle packing in square is applied for accounting amount of bubbles.



### 3.4 SOC and Recharge Efficiency

In order to terminate the recharge process, an important parameter, state of charge (SOC), must be continuously tracked. This parameter is defined as an indication of the amount of energy inside the battery compared to its maximum capacity. The SOC is mathematically expressed in equation (3.18) (Hussein and Fardoun 2015)

$$SOC_k = SOC_{K-1} + \eta \frac{i_k \Delta t}{C_T} \tag{3.18}$$

where $i_k$ is the current at instance $k$ (positive for discharging and negative for recharging), $\eta$ is the recharge efficiency, which can be obtained from manufacturer datasheet or found experimentally as given in equation (3.19), where $C_{\text{recharge}}$ is the recharge capacity (Ah):

$$\eta = \frac{C_{\text{recharge}}}{C_T} \tag{3.19}$$

here, we assume that the recharge efficiency is about 65%. However, calculation of recharge efficiency in this work is represented in another way as ratio of electrical energy to chemical energy which is expressed in equation (3.20):

$$\eta = \frac{E_{in}}{E_{acc}} \times 100\% \tag{3.20}$$

where $E_{in}$ is electrical energy which is energy input to battery. This energy can be calculated by multiple between current density and potential of battery whereas $E_{acc}$ is accumulated chemical energy in zinc element which is equal to formation energy.



### 3.5 Cycle stability

In general, the end of life for a battery is often defined as a capacity loss of more than 20% or an increase of the cell resistance by more than 100% (Keil and Jossen 2016). The key parameter which is used to determine the service life of battery is cycling stability. It is defined by the number of charging- or discharging cycles until its capacity is reduced to a certain amount of its nominal capacity or stable of recharging- or discharging voltage of each cycle

# Chapter IV
# Simulation and Validation

Descriptions of the model used in more detail including reaction rate of each electrode, mass balance of each component, and potential of the battery are presented in this chapter. Moreover, simulation procedure and a set of parameters applied in this work are also described.

## 4.1 Mathematical Model

According to the general form of equation which was presented in last chapter, expanded of zinc-air battery model is derived in this section.

### 4.1.1 Reaction rate

The reaction rate of reaction at zinc and air electrode are described with a Butler-Volmer approach. Both equation are adapted from Sunu and Bennion (1980) and Deiss, Holzer et al. (2002), respectively. As for the reaction rate of precipitating of solid zinc, the saturated approach is accounted, so that

$$r_I = -\begin{bmatrix} k_I^c \cdot \dfrac{c_{Zn(OH)_4^{2-}}^{zinc}}{c^{ref}} \cdot \exp\left(-\dfrac{(1-\alpha^{c,zinc})\cdot F}{R\cdot T}\cdot\eta^{zinc}\right) \\ -k_I^a \cdot \left(\dfrac{c_{OH^-}^{zinc}}{c^{ref}}\right)^4 \cdot \dfrac{n_{Zn}}{n^{ref}} \cdot \exp\left(\dfrac{\alpha^{a,zinc}\cdot F}{R\cdot T}\cdot\eta^{zinc}\right) \end{bmatrix} \quad (4.1)$$

$$r_{II} = k_{II}(c^{zinc}_{Zn(OH)^{2-}_4} - c^{sat}_{Zn(OH)^{2-}_4}) \tag{4.2}$$

$$r_{III} = \begin{bmatrix} \mathrm{k}^{a}_{III} \cdot \dfrac{c^{air}_{H_2O}}{c^{ref}} \cdot \left( \dfrac{c^{*}_{O_2}}{c^{ref}} \right)^{\frac{1}{2}} \cdot \exp\left( -\dfrac{(1-\alpha^{c,\mathrm{air}}) \cdot F}{R \cdot T} \cdot \eta^{air} \right) \\ -\mathrm{k}^{c}_{III} \cdot \left( \dfrac{c^{air}_{OH^-}}{c^{ref}} \right)^{2} \cdot \exp\left( \dfrac{\alpha^{a,\mathrm{air}} \cdot F}{R \cdot T} \cdot \eta^{air} \right) \end{bmatrix} \tag{4.3}$$

where $c^{*}_{O_2}$ is considered to be a concentration of dissolved oxygen present in liquid electrolyte at air electrode.

### 4.1.2 Mass balance equation

The molar concentration for species $k = OH^-,\ H_2O,\ Zn(\mathrm{OH})^{2-}_4$ and $K^+$ in the liquid electrolyte within electrode $j$, indicating either zinc or air electrode, is applied as equation (4.4). These concentrations are calculated with the following mass balance in concentration form as expressed in equation (3.10). Moreover, the volume change of the electrolyte at each electrode is presented in previous chapter.

$$c^{j}_{k} = \frac{n^{j}_{k}}{V^{j}_{electrolyte}} \tag{4.4}$$

As for solid zinc and zinc oxide, there is no zinc allowed to enter or leave the system. The amount of converted solid zinc is expressed by an algebraic equation

as equation (4.5). In addition, the accumulation of solid zinc oxide is expressed by equation (4.6)

$$n_{Zn} = n_{Zn}^{total,t=0} - n_{ZnO} - n_{Zn(OH)_4^{2-}}^{zinc} - n_{Zn(OH)_4^{2-}}^{air} \tag{4.5}$$

$$\frac{dc_{ZnO}}{dt} = \nu_{ZnO} r_{II} \tag{4.6}$$

For the concentration of dissolve oxygen, the uptake oxygen is described as diffusion and absorption process determined by the air electrode, so that the concentration of oxygen change with time as following equation

$$\frac{dc_{O_2}^*}{dt} = \frac{\nu_{O_2 III} \cdot r_{III} + J_{O_2}^{bulk} - c_{O_2}^* \cdot \frac{dV_{electrolyte}^{air}}{dt}}{V_{electrolyte}^{air}} \tag{4.7}$$



where $J_{O_2}^{bulk}$ is represented by balancing the molar flows of oxygen in KOH electrolyte as shown in equation (4.8)

$$J_{O_2}^{bulk} = -D_{O_2,KOH} \cdot \frac{c_{O_2}^* - c_{O_2}^{*GDL}}{\delta_{film}^{air}} \cdot A_{free}^{GDL} \tag{4.8}$$

The concentration of oxygen at electrolyte interface, $c_{O_2}^{*GDL}$ depends on electrolyte concentration and partial pressure in the gas diffusion layer (GDL). A

suitable Henry-type relation, which is calculated by Fick's diffusion, is given by Tromans (1998). This relation is used to calculated $c_{O_2}^{*GDL} \cdot p_{O_2}^{GDL}$ in this work and a linear profile of the relation from constant oxygen partial pressure at environment, $p_{O_2,env}$, through the GDL with a thickness of film, $\delta_{film}^{GDL}$, and area, $A_{free}^{GDL}$.

## 4.2 Parameters

A set of designed parameters like material properties and environmental parameters, which are applied in this simulation, are given in Table A.1 with their respective literature references.

## 4.3 Simulation procedure

### 4.3.1 Effect of recharge current density on oxygen evolution rate

All presented simulations are obtained for continuous galvanic cycle which begin with recharging process and then followed by discharging process. The conditions of both process are 6 hours at current density $i^{cell} = -0.9\ A\ dm^{-2}$ (the negative sign represent recharging process) and 3 hours at current density $i^{cell} = 1.8\ A\ dm^{-2}$, respectively. After that, the performance of recharging process of next cycle which begin with 50% SOC is studied. The respective initial conditions of this simulation at time, $t = 0$ at operating temperature are shown in Table A.2.

It appears that recharging with 6 hours at $i^{cell} = -0.9\ A\ dm^{-2}$ cannot full fill the SOC of the battery. Hence, the strategy of recharging process should be

investigated. Two-stage constant current and multi-stage constant current recharge pattern may enhance the recharging process of this battery and reach 100% SOC. In addition, a length of the battery lifetime can be increased due to this strategy.

Generally, the recharging time, which depends on recharged current and capacity of the battery, of 10 Ah battery can be reach fully recharge in 12-16 hours with 1 Ah recharged current. This charging time is moderately long and becomes impractical when fast recharges are needed. Therefore, the strategy should provide complete recharging in less than 8 hours due to cycling stability (Li, Gong et al. 2013). Moreover, its recharging efficiency is acceptable at more than 65%.

### 4.3.2 Cycle life

It is important to notice the cycle stability of the battery for the reason that it reflects the cycle life of battery. In general, the cycle life is influenced more by high charging currents. Different boost charging protocols have disclosed that high charging currents can deteriorate cycle life. In this work,



### 4.3.3 Side reaction

At potentials above standard cell potential of other reactions, side reactions become thermodynamically favorable. These reactions are detrimental to the life and safety of Li-ion cells. In general, they dictate many aspects of battery behavior.

As for side reaction, water electrolysis reaction which is side reaction of zinc-air battery, can occur during recharging process. At potentials above 1.23 V, this reaction becomes thermodynamically favorable. It is detrimental to the life of battery and it also dictates the recharging performance of the battery. Especially,

cycle life of battery and recharging efficiency are two main things that are affected from side reaction.

All equations which represent the model in this work are implemented in Matlab and solved with the ode15s ODE solver on an Intel(R) Core(TM) i5-2410M CPU, 64 bit Operating System with 4GB RAM.

# Chapter V
# Results and Discussion

This chapter presents effect of current density on oxygen growth and other simulation results which perform the recharging performance of zinc-air battery are also present. In addition, these simulation results are validated by comparing with published experimental data. Moreover, the recharging strategies to avoid those effects are shown in this chapter.

## 5.1 Validation

The results of simulation in this work were validated by comparing the polarization curve for both discharging and recharging processes of the zinc-air batteries with the published results of Deiss, Holzer et al. (2002) as illustrate in Figure 5.1. It can be observed that the simulated results and experimental data are in-line within a margin of few mV. Thus, the developed model can be used to investigate the recharging performance of zinc-air battery at various different recharging policies.

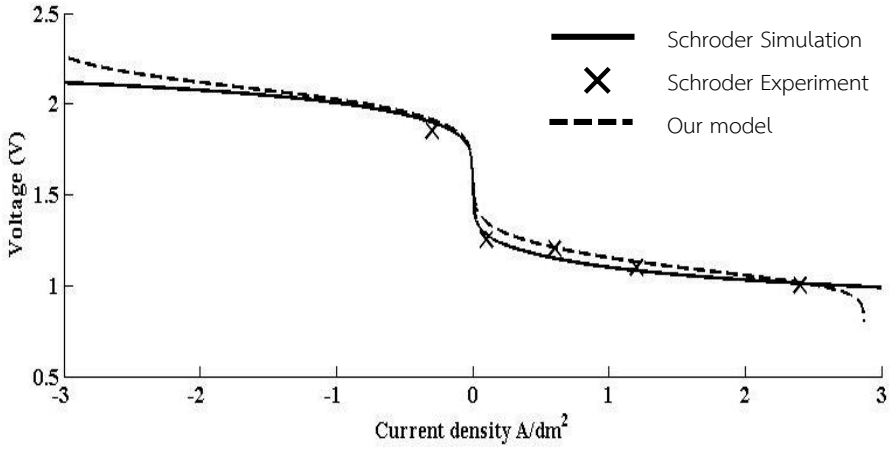


**Figure 5.1** Validation of polarization between simulation results and experimental result.

## 5.2 Effect of recharged current density on oxygen evolution rate

Oxygen evolution reaction (OER) in recharging process is limitation of this type of battery because it can generate many bubbles which can gather and adhere the electrode. The OER at air electrode is blocked by those bubbles adhered to the electrode.

The model of bubble was developed and applied in this work to study performance of battery during recharging process. Parameters of bubbles behavior in KOH electrolyte, which are characterized by Janssen, Sillen et al. (1984), such as radius of bubble and bubble population density. These parameter are used to compare with bubble model in simulation results for reasonable and realistic of the model.

The cycle stability of the battery model which is assumed that no effect of oxygen evolution is shown in Figure 5.2. Also, the model including effect of oxygen evolution is plotted in this figure. It is apparent that effect of oxygen evolution contribute instability in battery cycle and low cycle life of the battery about 4 cycle, approximately. Beside, mass balance of all species in zinc-air battery system is plotted as ratio in Figure 5.3 to 5.6 including water and hydroxide ion at both side of electrode in each cycle. Moreover, mole zinc in each cycle is also shown in Figure 5.7. It was found that water balance of Schroder model at both electrodes are less obviously than those of oxygen model in this work due to lack of oxygen during discharge for reacting with water. Also, water cannot react with oxygen during recharge is another reason for increasing of water in this system.

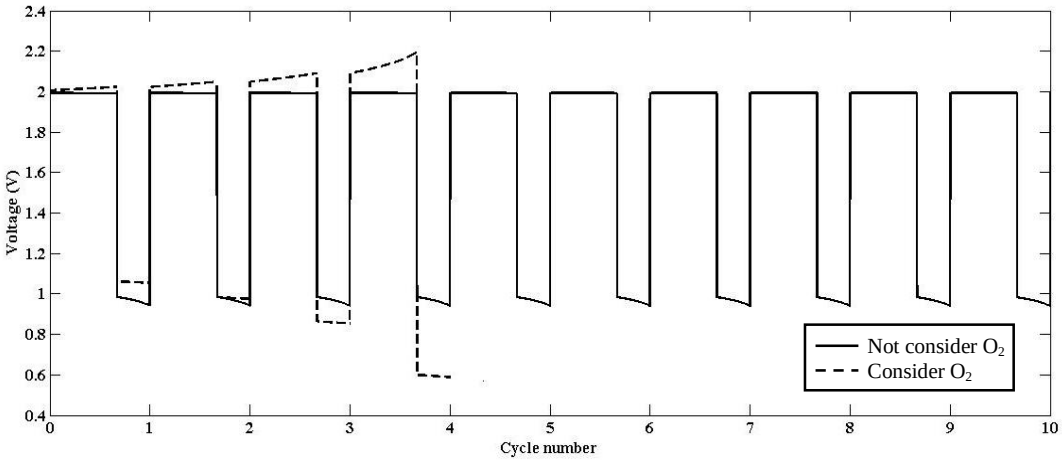


**Figure 5.2** Cycling data of zinc-air battery model

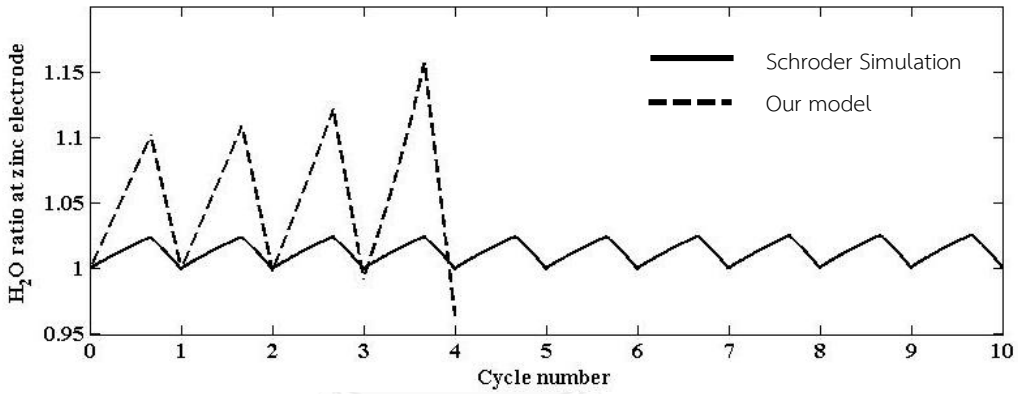


**Figure 5.3** Water ratio at zinc electrode of oxygen bubble model result compared with Schroder result.

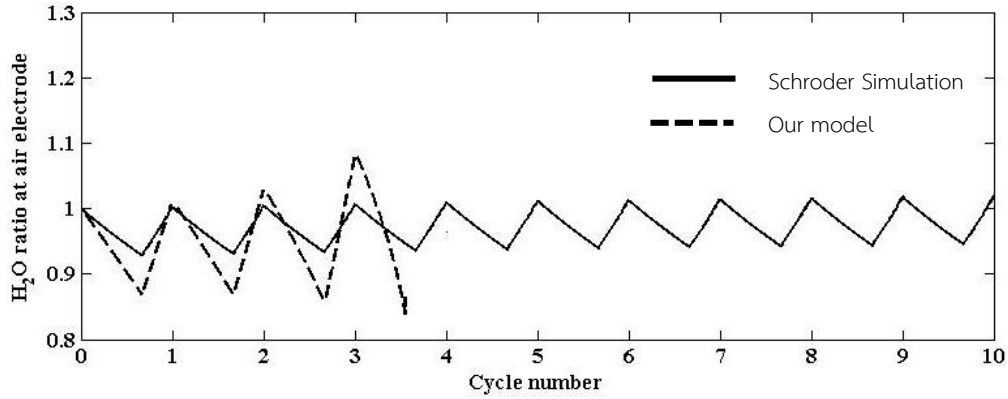


**Figure 5.4** Water ratio at air electrode of oxygen bubble model result compared with Schroder result.

As for hydroxide ion, it was apparent that mole of hydroxide at both sides of electrode of oxygen model loss during cycle according to shortage of product of oxygen reduction reaction as discharge cycle of battery. Another reason is slow rate reaction of oxygen evolution reaction during recharge cycle.

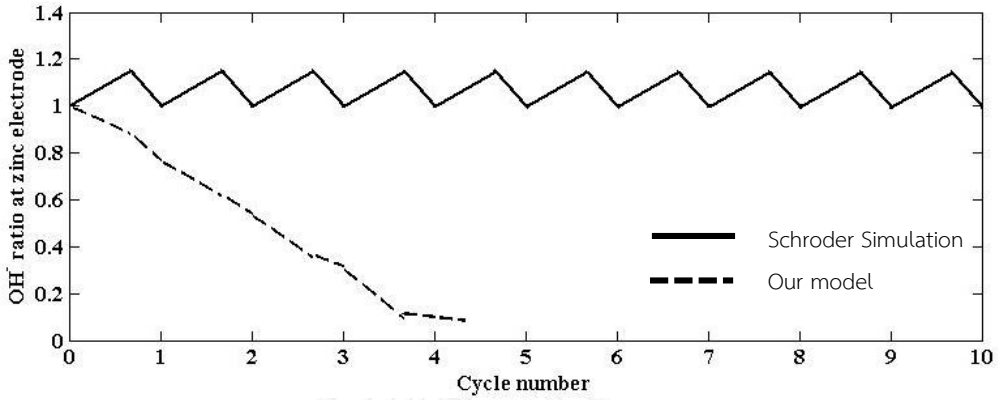


**Figure 5.5** Hydroxide ion ratio at zinc electrode of oxygen bubble model result compared with Schroder result.

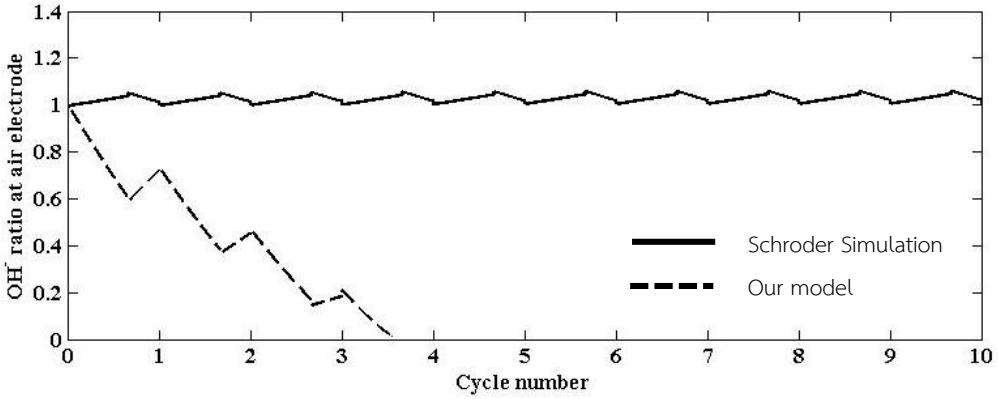


**Figure 5.6** Hydroxide ion ratio at air electrode of oxygen bubble model result compared with Schroder result.

For mass balance of zinc, it seems that rate of generation and consumption of zinc in our model is less than that of Schroder model because of bubbles which decrease reactive area at recharging electrode of this system.

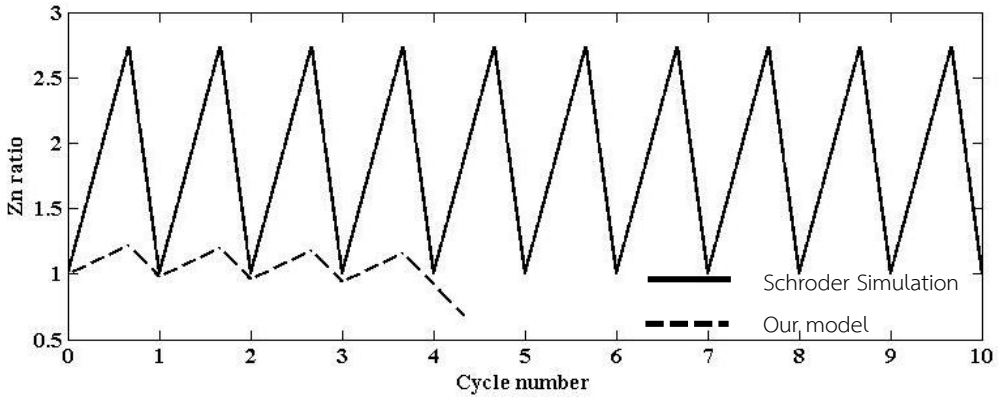


**Figure 5.7** Zinc ratio of oxygen bubble model result compared with Schroder result.

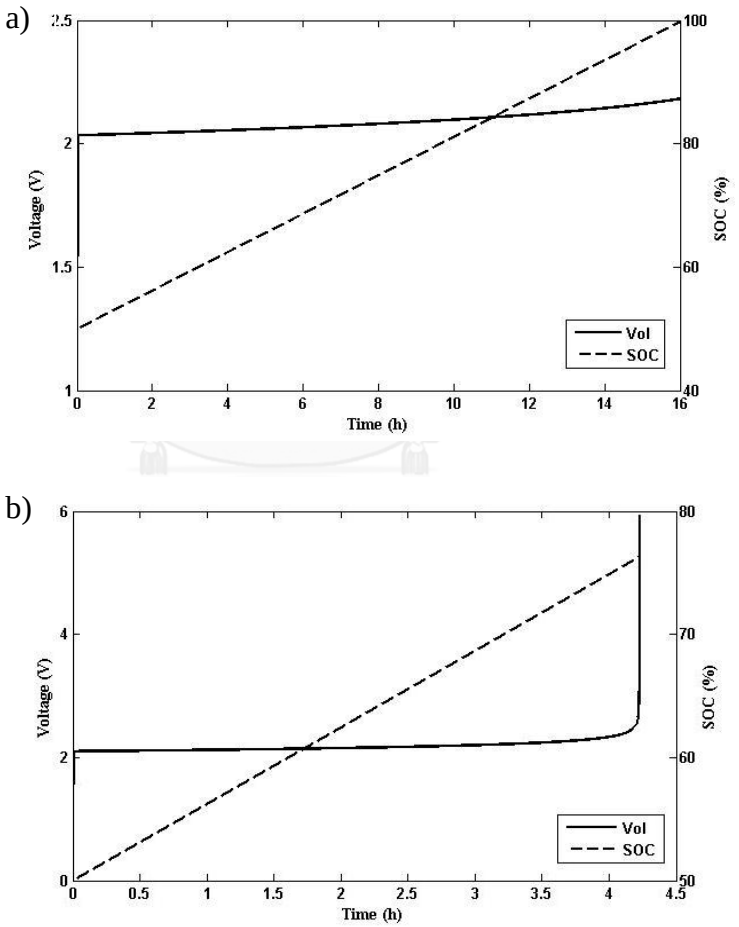


**Figure 5.8** Voltage and SOC of battery versus time a).recharge with $i^{cell} = -1\ A\ dm^{-2}$, b).recharge with $i^{cell} = -2\ A\ dm^{-2}$.

In this study, current density which is used in recharging process is in range $0.6-1\,Adm^{-2}$ due to cycling stability in long recharge period (Li, Gong et al. 2013). These current magnitude can provide 100% SOC but use more than 8 hours to reach fully recharge. It can be seen that the voltage slightly increases during the recharging period may as a result of oxygen bubbles growth which can block reaction at recharge electrode as shown in Figure 5.8 a). However these bubbles are not much enough to completely block the reaction or stop the recharging process before reach 100% SOC.

To shorten recharging time, a higher magnitude recharging current density must be used but using this value leads to a higher rate of oxygen evolution reaction which generate many bubbles. These bubbles are able to stop recharging process before battery become fully recharge by totally prevent the reaction at recharge electrode as depicted in Figure 5.8 b). Stopping of recharging process may be indirectly reflected by sharp increase of recharging voltage signal. It can be observed that the cell voltage increase sharply because of over potential at recharge electrode (air electrode) as displayed in Figure 5.9.



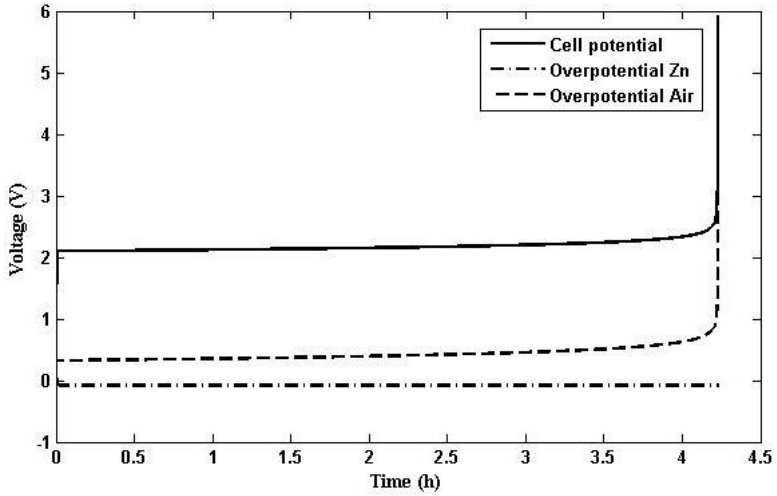


**Figure 5.9** Cell potential including over potential at zinc and air electrode.

Thus, there should be the recharge protocol that can overcome the bubble problem during recharging process and produce cycling stability to the battery. Two-stage constant current is conducted to solve the problems by using different magnitude of current density at each stage of the process. According to Li, Gong et al. (2013), current density in magnitude range $0.6-1\ Adm^{-2}$ are used to recharge zinc-air battery in long period which contribute long cycle life and cycling stability. Another range is $2\ Adm^{-2}$ which is used for recharging in short period as for the same reasons as the previous range.

In this section, effect of magnitude of constant current density on oxygen evolution rate is studied and ranges of current density are similar to the mentioned above. The rates of oxygen evolution at various current densities during beginning of recharge process are plotted in Figure 5.10. It's clearly seen that oxygen concentration, which is stand for its evolution rates, rises significantly as recharging current density increases. Apparently, the higher oxygen concentration, the more amount of bubbles because there is a few solubility of oxygen gas in alkaline electrolyte result in forming of oxygen bubbles from insoluble gas. This seems to may imply that high magnitude of current density can reach 100% SOC of battery faster than that low magnitude but it also has more opportunity to fail the recharge process due to blocking reaction at recharge electrode of bubbles than the low magnitude.

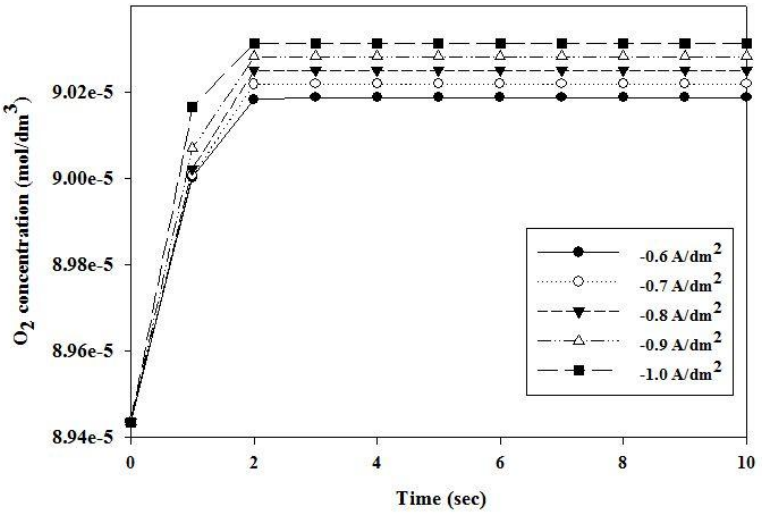


**Figure 5.10** Oxygen evolution rate versus current density in magnitude range $0.6-1\,Adm^{-2}$.

The oxygen concentration may result in recharging performance of the battery including recharging time and recharging efficiency which is reflected by energy loss. Figure 5.11 shows both of them at different recharging current density. It was found that ranges of current density which are used in this work, $0.6-1\,Adm^{-2}$ and around $2\,Adm^{-2}$, are suitable for two-stage recharge protocol because the former range contribute less energy loss than 20% that mean recharging efficiency is guaranteed up to 80% and the latter range provide short recharging time significantly about 4 hours. These two ranges will be used in recharging strategies in next section.

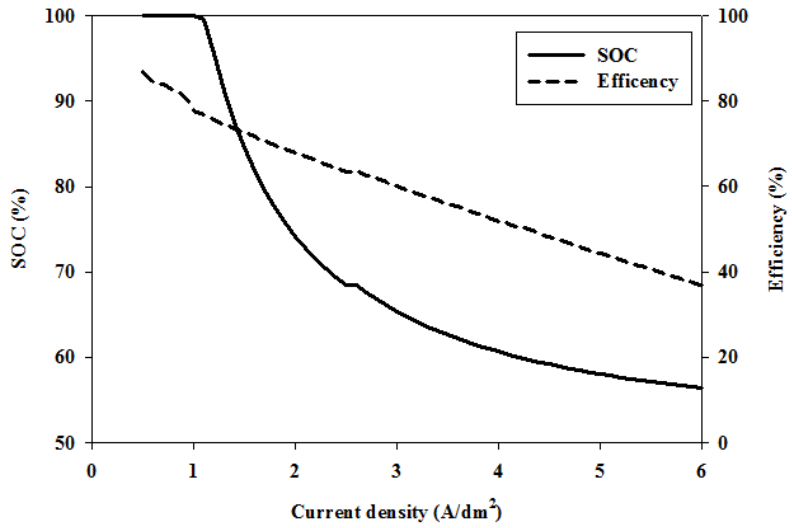


**Figure 5.11** Recharging time versus Energy loss.

## 5.3 Recharge strategies

The recharging performance of second cycle of the zinc-air battery using different recharging policies is studied. Two-stage constant current is a one strategy which is commonly used to recharge battery (Keil and Jossen 2016). The criteria of this strategy is regulated recharging voltage. At first, the first stage of this recharging process will be end if the recharging voltage be at 2.3V. This value is determined by the air cathode limitation of zinc-air battery, OER which affects to the hydroxide ions. It could be indicated that the recharging voltage rise up rapidly when those ions dry out as can be seen in Figure 5.12. After finishing of first stage, the second stage of this recharging process is conducted.

Table 5.1 shows different recharging patterns of two-stage constant current recharge strategy which are able to reach 100% SOC. It was found that recharging efficiency of each pattern were comparable. As for the recharging time, it could be concluded that the recharging time of the patterns, which used the same magnitude of

current at first stage, depend on current magnitude of the second stage. The time declined obviously as the magnitude of second stage increased.

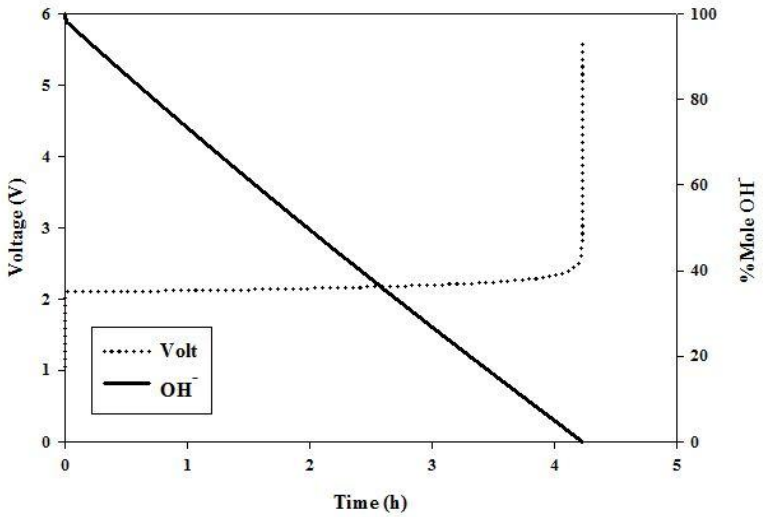


**Figure 5.12** Limitation of OER indicated by hydroxide ions and recharging voltage.

**Table 5.1** Recharging performance of two-stage constant current recharging strategy

| Recharging pattern | Recharging time (h) | | | Recharging efficiency |
|---|---|---|---|---|
| | First | Second | Total | |
| 1). $2\,A/dm^2 + 0.6A/dm^2$ | 3.9 | 2 | 5.9 | 69.0% |
| 2). $2A/dm^2 + 0.7A/dm^2$ | 3.9 | 1.7 | 5.6 | 68.9% |
| 3). $2A/dm^2 + 0.8A/dm^2$ | 3.9 | 1.5 | 5.4 | 68.8% |
| 4). $2.1A/dm^2 + 0.6A/dm^2$ | 3.5 | 2.8 | 6.3 | 68.8% |
| 5). $2.1A/dm^2 + 0.7A/dm^2$ | 3.5 | 2.4 | 5.9 | 68.6% |
| 6). $2.2A/dm^2 + 0.6A/dm^2$ | 3.1 | 3.5 | 6.6 | 68.6% |

On the other hand, the pattern used the similarity of the second current magnitude, recharging time depended on those in the first stage. Interestingly, recharging time increased when the magnitude of current density in first stage increased. These may result from high amount of bubbles which are generated by high oxygen concentration. The example of current density and voltage profile of two-stage constant current pattern is plotted in Figure 5.13.

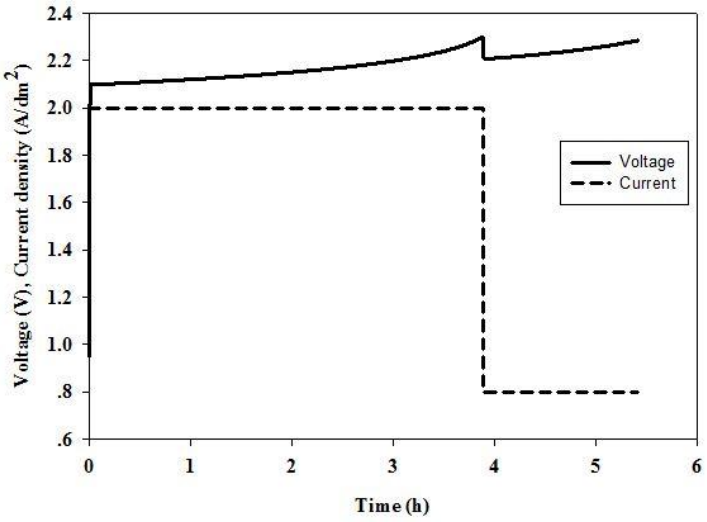


**Figure 5.13** Recharging profile, voltage and current density, of two-stage pattern 3.



One of the benefit of this recharge protocol is that it has a potential to produce the cycling stability of the battery as illustrated in Figure 5.14. It is evident from the result that this recharge strategy has more cycling stability compared with normal recharge in the battery model which considers effect of oxygen evolution.

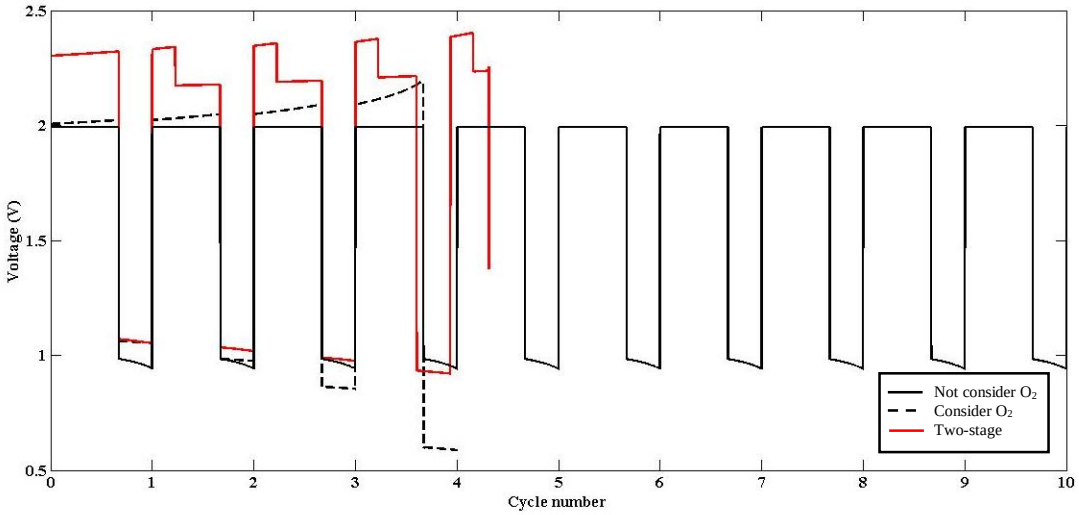


**Figure 5.14** Cycling data of two-stage constant current recharge strategy.

Another strategy which is commonly used for recharge the battery is multi-stage constant current. This strategy has an advantage in recharging time because of variety of magnitude of recharging current density. In this section, the recharging patterns are able to provide 100% SOC at the end of recharging process are investigated. The performances of these patterns are summarized in Table 5.2.

**Table 5.2** Recharging pattern of multi-stage constant current

| Recharging Pattern ($A/dm^2$) | Recharging time (h) | Recharging efficiency |
|---|---|---|
| 2+1.6+1.5+1.3+1.1 | 3.89+0.14+0.04+0.1+0.15 = **4.32** | 68% |
| 2.1+1.8+1.6+1.4+1.3+ 1.2+1.1+1.0+0.9+0.8+ 0.7+0.6 | 3.50+0.08+0.07+0.09+0.05+0.06+0.07+ 0.09+0.11+0.14+0.18+0.01 = **4.45** | 67% |
| 2.2+2.0+1.9+1.7+1.5+ 1.2+1.0+0.9+0.8+0.7+ 0.6+0.5+0.4 | 3.15+0.04+0.03+0.06+0.08+0.18+0.17+ 0.11+0.13+0.17+0.23+0.33+0.18 = **4.86** | 66% |

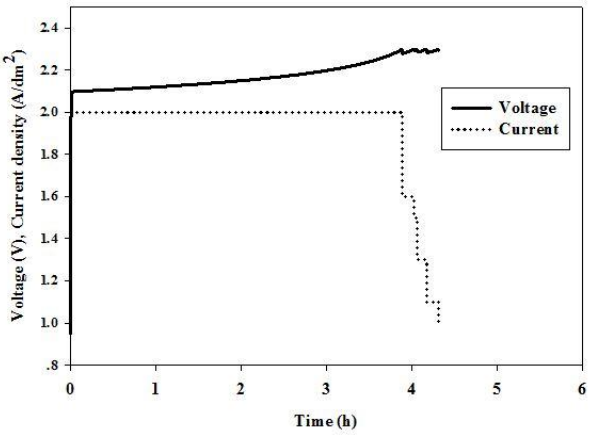


**Figure 5.15** Recharging profile, voltage and current density, of multi-stage pattern 1.

Similar results as previous strategy were found in this strategy, the recharging time increased imperceptibly as recharging pattern began with high magnitude current density whereas the efficiencies vary but not significantly. Furthermore, the example of some pattern in this strategy is plotted in Figure 5.15. It can be observed that the recharging voltage is steadily at 2.3V result from voltage regulation as discussed previously. Moreover, this also affect significantly to the cycling stability of the battery as same as two-stage constant current strategy.



## 5.4 Side reaction

Due to water has its electrochemically stable below -0.82 V vs SHE (standard hydrogen potential), this leads to water electrolysis reaction during recharging process of zinc-air battery. In this system, the overall hydrogen evolution reaction is shown to proceed by alkaline water electrolysis pathway. However, the reverse reaction of this reaction can be neglected due to the low (rather negative) potentials prevailing at a zinc electrode in the zinc-air battery (Deiss, Holzer et al. 2002). Therefore, the effect of this unwanted side reaction is able to result in recharging process only.

In general, the side reaction occur during recharging process hardly even though its standard cell potential is low enough but the electrochemical rate constant of hydrogen evolution reaction (HER) (equation (3.4)) is not high adequately compared with the electrochemical rate of regenerated zinc. The evidence of this result is shown in Figure 5.16.

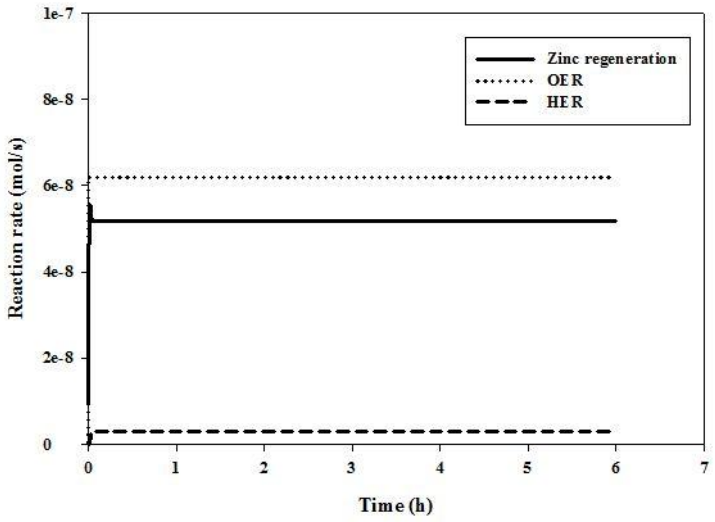


**Figure 5.16** Rate reaction during recharging process at zinc and air electrode.



Anyway, if the side reaction occur, its effects are appeared that the recharging performance and cycle life of the battery are deteriorated. These effects are represented by recharging voltage and mass of reactant and product of zinc regeneration reaction (reverse reaction of equation (3.1)). As shown in Figure 5.17, the recharging voltage of side reaction model changes insignificantly compared with that of oxygen bubble model. In addition, this side reaction effect on cycle stability of the battery which is shown in Figure 5.18 is also studied. Obviously, the cycling stability is similar to that of oxygen bubble model so, this effect is not considered in recharging strategies.

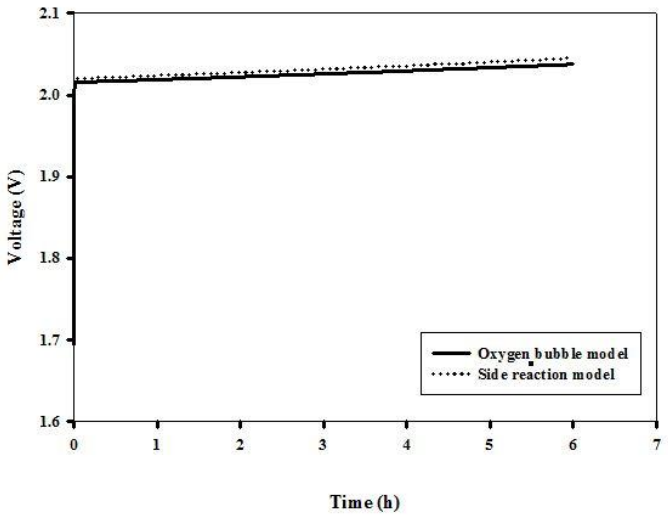


**Figure 5.17** Recharging voltage of both oxygen bubble model and side reaction model.

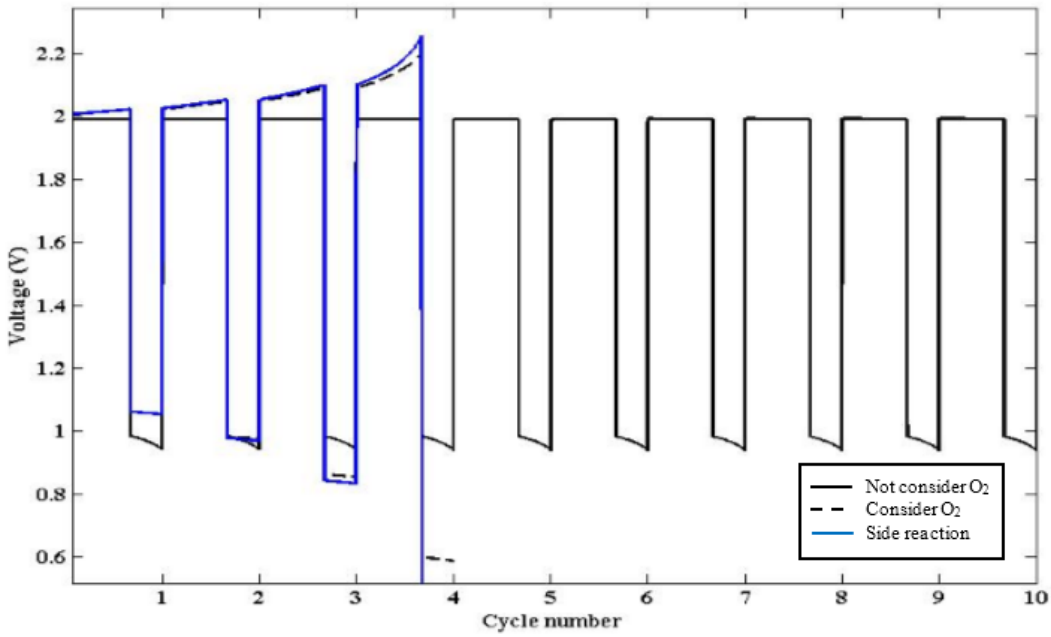


**Figure 5.18** Cycling data of side reaction model.

Another effect of this side reaction is a decrease of water which is reactant of zinc regeneration reaction result in a decrease of regenerated metal zinc. The profile of water and zinc which are recharged with $0.9\ A/dm^2$ in oxygen bubble model and side

reaction model are plotted in Figure 5.19 and 5.20, respectively. Moreover, the effect of different recharging current density on water consumption rate and zinc regeneration rate are studied and plotted in those Figures as well. Apparently, rate of water consumption of side reaction model is greater than that in oxygen bubble model as could be seen in Figure 5.19. In addition, recharging with high magnitude current density definitely rises the consumption rate of water as same as low magnitude which could decrease that rate of water.

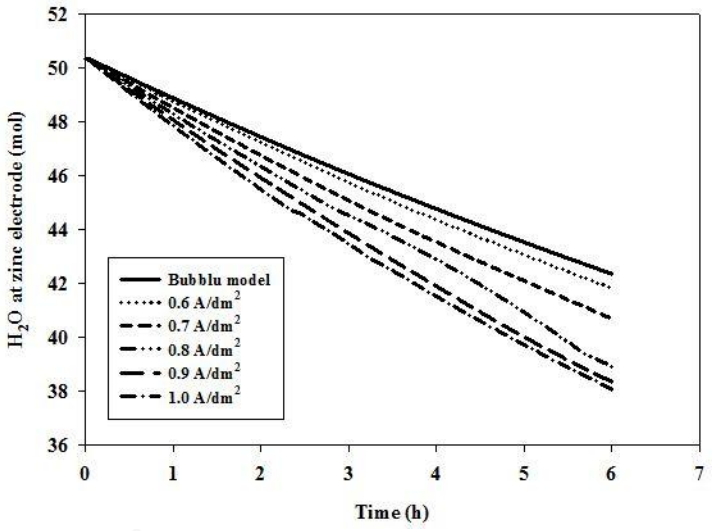


**Figure 5.19** Consumption rate of water of side reaction model at zinc electrode.

As for a metal zinc product, rate of the regenerated zinc decreases when side reaction is considered in the model despite using recharging current density identically, $0.9\,A/dm^2$, as illustrated in Figure 5.20. Furthermore, the results of effect of recharging current density magnitude on zinc regeneration rate is also shown in this graph. This effect result from water consumption rate that is the regeneration rate falls while magnitude of recharging current density increases.

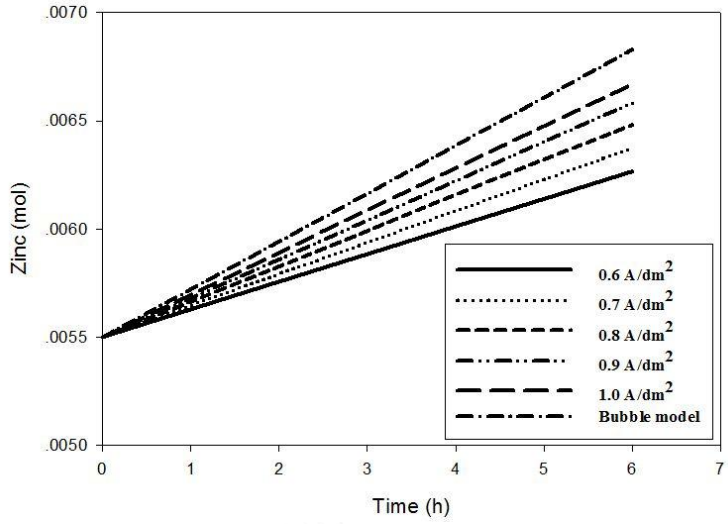


**Figure 5.20** Generation rate of metal zinc of side reaction model at zinc electrode.

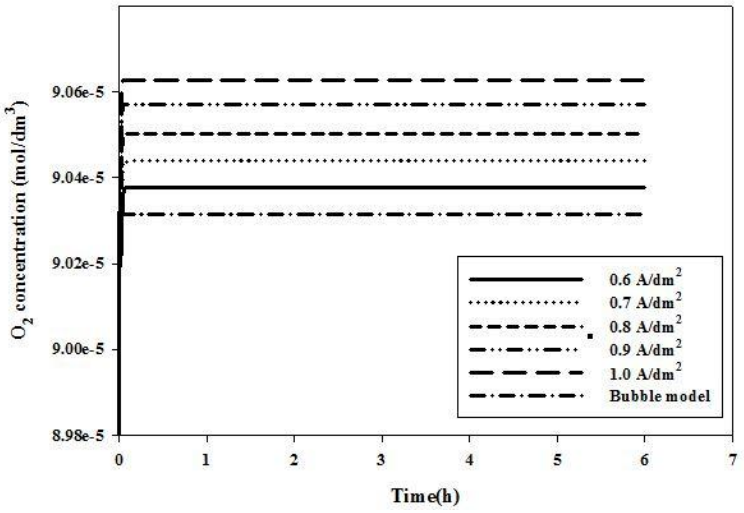


**Figure 5.21** Oxygen evolution rate of side reaction model.

Turning to another product of water electrolysis reaction, the oxygen evolution of both oxygen bubble model and side reaction model which are recharged with similar current density are compared in Figure 5.21. It can be seen that even though the recharged current density are alike, the oxygen evolution rate of side reaction model is higher abundantly than that of oxygen bubble model. Also, the effect of magnitudes of

current density on oxygen evolution rate are plotted in this Figure. The effect of current density on oxygen evolution rate are the same as explained in the previous section. As for the hydrogen evolution, the bubbles from hydrogen are not accounted in the bubble model due to its high solubility in potassium hydroxide electrolyte. Even though, the dissolved hydrogen may cause self-discharge of zinc-air battery during discharge cycle.

However, these effects, cycling stability and decrease of reactant and product mass even oxygen evolution from water electrolysis, are not significantly in low cycle life battery or small scale battery. Therefore, the effect of oxygen bubble during recharging process is only considered in the strategies for zinc-air battery in this work.

# Chapter VI
# Conclusion and Recommendation

## 6.1 Conclusion

A mathematical model of zinc-air battery is applied via Matlab software and also used to study behavior of battery during recharging process including mass balance of chemical substances. In addition, the recharging performance of the battery is studied as well. The effects of oxygen bubble evoultion and side reaction during recharging process of zinc-air battery are also studied. In addition, the two-stage and multi-stage constant current density recharging strategies are investigated to handle these effects.

As for the result of this research, the simulation result of polarization characteristic is compared with published experimental data for validation. Clearly, this model is suitable for predicting the battery due to simulated results and experimental data are in-line within a margin of little errors.

In summary, the current density affect significantly to oxygen evolution rate which results in bubbles growth and lead to blocking reaction at recharging electrode. The two-stage and multi-stage recharging strategies are able to eliminate this problem with short recharging time and high efficiency. Moreover, these strategies allow the cycling stability to the battery. On the subject of side reaction, effects of this side reaction on recharging performance and cycling stability of the battery are studied as well. It could be found that the recharging voltage slightly changed but not affect to stable of each cycle of battery. In addition, the regenerated metal zinc marginally fall and the water substance low decrease compared with the model that side reaction is not

considered. However, it is appeared that the side reaction not contribute effect to the small scale battery insignificantly.

## 6.2 Recommendation

For reasonable recharging strategy, scale up battery and optimization strategy should be investigated. In addition, other problems during recharging process such as dendrite growth of metal zinc should be accounted. As for result validation, the experiment of recharging process of zinc-air battery for this study should be set up if possible.

## REFERENCES


Abdollahi, A., et al. (2016). "Optimal battery charging, Part I: Minimizing time-to-charge, energy loss, and temperature rise for OCV-resistance battery model." Journal of Power Sources **303**: 388-398.

Arise, I., et al. (2010). "Numerical Calculation of Ionic Mass-Transfer Rates Accompanying Anodic Zinc Dissolution in Alkaline Solution." Journal of Electrochemical Society **157**(2): 8.

Bird, E., et al. (2002). Transport phenomena, Applied Mechanics Reviews.

Bockris, J. O. M. and T. Otagawa (1984). "The Electrocatalysis of Oxygen Evolution on Perovskites." Journal of Electrochemical Society **131**(2): 13.

Cope, R. C. and Y. Podrazhansky (1999). The art of battery charging. Battery Conference on Applications and Advances, 1999. The Fourteenth Annual.

Daniel Schröder and Ulrike Krewer (2014). "Model based quantification of air-composition impact on secondaryzinc air batteries." Electrochimica Acta **117**(2014): 13.

Deiss, E., et al. (2002). "Modeling of an electrically rechargeable alkaline Zn-air battery." Electrochimica Acta **47**(2002): 16.

Dirkse, T. P., et al. (1968). "The Anodic Behavior of Zinc in KOH Solutions." Journal of Electrochemical Society **115**(5): 3.

Grew, K. N., et al. (2011). "Effects of Temperature and Carbon Dioxide on Anion Exchange Membrane Conductivity." Journal of Electrochemical Society **14**(12): 5.

Hussein, A. A. and A. A. Fardoun (2015). "Design considerations and performance evaluation of outdoor PV battery chargers." Renewable Energy **82**(2015): 7.

Ikeya, T., et al. (2002). "Multi-step constant-current charging method for an electric vehicle nickel/metal hydride battery with high-energy efficiency and long cycle life." Journal of Power Sources **105**(1): 6-12.

Ikeya, T., et al. (1998). "Multi-step constant-current charging method for electric vehicle, valve-regulated, lead/acid batteries during night time for load-levelling." Journal of Power Sources **75**(1): 101-107.

Janssen, L. J. J., et al. (1984). "Bubble behaviour during oxygen and hydrogen evolution at transparent electrodes in KOH solution." Electrochimica Acta **29**(5): 633-642.

Keil, P. and A. Jossen (2016). "Charging protocols for lithium-ion batteries and their impact on cycle life—An experimental study with different 18650 high-power cells." Journal of Energy Storage **6**: 125-141.

Kimble, M. C. and R. E. White (1991). "A Mathematical Model of a Hydrogen/Oxygen Alkaline Fuel Cell." Journal of Electrochemical Society **138**(11): 13.

Krej, I., et al. (1993). "Transport of Zn (OH) - Ions across a Polyolefin Microporous Membrane." Journal of Electrochemical Society **140**: 5.

Li, Y. and H. Dai (2014). "Recent advances in zinc–air batteries." Chemical Society Reviews **43**(2014): 19.

Li, Y., et al. (2013). "Advanced zinc-air batteries based on high-performance hybrid electrocatalysts." Nat Commun **4**: 1805.

Mathias, P. M. (2004). "Correlation for the Density of Multicomponent Aqueous Electrolytes." Industrial & Engineering Chemistry Research **43**(19): 6.

Qiao, J., et al. (2013). "Effect of KOH Concentration on the Oxygen Reduction Kinetics Catalyzed by Heat-Treated Co-Pyridine/C Electrocatalysts." international Journal of Electrochemical Science **8**(1): 20.

Riietschi, P. (1967). "Solubility and Diffusion of Hydrogen in Strong Electrolytes and the Generation and Consumption of Hydrogen in Sealed Primary Batteries." Journal of Electrochemical Society **114**(4): 5.

Sapkota, P. and H. Kim (2009). "Zinc–air fuel cell, a potential candidate for alternative energy." Journal of Industrial and Engineering Chemistry **15**(4): 445-450.

Sunu, W. G. and D. N. Bennion (1980). "Transient and Failure Analyses of the Porous Zinc Electrode: II . Experimental." Journal of Electrochemical Society **127**(9): 9.

Tromans, D. (1998). "Oxygen solubility modeling in inorganic solutions: concentration, temperature and pressure effects." Hydrometallurgy **50**(3): 279-296.

Wang, K., et al. (2015). "Growth of oxygen bubbles during recharge process in zinc-air battery." Journal of Power Sources **296**(2015): 6.

Xu, M., et al. (2015). "Rechargeable Zn-air batteries: Progress in electrolyte development and cell configuration advancement." Journal of Power Sources **283**(2015): 14.

Zhou, G., et al. (2011). "Effects of property variation and ideal solution assumption on the calculation of the limiting current density condition of alkaline fuel cells." Journal of Power Sources **196**(11): 4923-4933.

# APPENDIX

**Table A.1** Applied parameters for this work

| parameter | value | unit | source |
|---|---|---|---|
| $\in^{sep}$ | 0.41 | - | Daniel Schröder and Ulrike Krewer (2014) |
| $\in^{GDL}$ | 0.5 | - | Daniel Schröder and Ulrike Krewer (2014) |
| $\delta_{electrode}^{zinc}$ | 0.13 | $dm$ | Daniel Schröder and Ulrike Krewer (2014) |
| $A_{electrode}^{zinc}$ | $1.33\times10^{-2}$ | $dm^2$ | Daniel Schröder and Ulrike Krewer (2014) |
| $\delta^{sep}$ | $2.5\times10^{-4}$ | $dm$ | Daniel Schröder and Ulrike Krewer (2014) |
| $A^{sep}$ | $1.33\times10^{-2}$ | $dm^2$ | Daniel Schröder and Ulrike Krewer (2014) |
| $\delta_{electrode}^{GDL}$ | $2.00\times10^{-3}$ | $dm$ | Daniel Schröder and Ulrike Krewer (2014) |
| $\delta_{film}^{air}$ | $5.00\times10^{-7}$ | $dm$ | Zhou, Chen et al. (2011) |
| $A_{free}^{GDL}$ | $7.85\times10^{-5}$ | $dm^2$ | Daniel Schröder and Ulrike Krewer (2014) |
| $A_{electrode}^{air}$ | $1.33\times10^{-2}$ | $dm^2$ | Daniel Schröder and Ulrike Krewer (2014) |
| $\sigma_{Zn}$ | $2.00\times10^{6}$ | $Sdm^{-1}$ | Sunu and Bennion (1980) |
| $\sigma_{ZnO}$ | $1.00\times10^{-9}$ | $Sdm^{-1}$ | Sunu and Bennion (1980) |
| $\tilde{V}_{Zn}$ | $9.15\times10^{-3}$ | $dm^3mol^{-1}$ | Sunu and Bennion (1980) |
| $\tilde{V}_{ZnO}$ | $1.45\times10^{-2}$ | $dm^3mol^{-1}$ | Sunu and Bennion (1980) |
| $\tilde{V}_{Zn(OH)_4^{2-}}$ | $1.86\times10^{-2}$ | $dm^3mol^{-1}$ | Daniel Schröder and Ulrike Krewer (2014) |
| $\tilde{V}_{H_2O}$ | $1.78\times10^{-2}$ | $dm^3mol^{-1}$ | Kimble and White (1991) |
| $\tilde{V}_{OH^-}$ | $7.89\times10^{-3}$ | $dm^3mol^{-1}$ | Mathias (2004) |
| $C_{DL}^{zinc}$ | 250 | $Fdm^{-1}$ | Dirkse, Wit et al. (1968) |
| $C_{DL}^{air}$ | 1.4 | $Fdm^{-1}$ | Bockris and Otagawa (1984) |
| $D_{Zn(OH)_4^{2-}}$ | $8.55\times10^{-9}$ | $dm^2s^{-1}$ | Krej, Van et al. (1993) |
| $D_{OH^-}$ | $4.94\times10^{-7}$ | $dm^2s^{-1}$ | Grew, Ren et al. (2011) |
| $D_{K^+}$ | $1.20\times10^{-7}$ | $dm^2s^{-1}$ | Sunu and Bennion (1980) |
| $D_{KOH}$ | $1.20\times10^{-7}$ | $dm^2s^{-1}$ | Arise, Kawai et al. (2010) |
| $D_{H_2O}$ | $5.26\times10^{-7}$ | $dm^2s^{-1}$ | Grew, Ren et al. (2011) |
| $D_{H_2O}^{GDL}$ | $2.59\times10^{-3}$ | $dm^2s^{-1}$ | Bird, Stewart et al. (2002) |
| $D_{O_2,KOH}$ | $7.50\times10^{-4}$ | $dm^2s^{-1}$ | Qiao, Xu et al. (2013) |
| $D_{H_2,KOH}$ | $1.20\times10^{-3}$ | $dm^2s^{-1}$ | Riietschi (1967) |
| $c_{Zn(OH)_4^{2-}}^{sat}$ | 0.66 | $mol\ dm^{-3}$ | Sunu and Bennion (1980) |

**Table A.1** Applied parameters for this work (continue)

| parameter | value | unit | source |
|---|---|---|---|
| $k_I^a$ | $4.78\times10^{-11}$ | $mol\ s^{-1}$ | Daniel Schröder and Ulrike Krewer (2014) |
| $k_I^c$ | $3.58\times10^{-8}$ | $mol\ s^{-1}$ | Daniel Schröder and Ulrike Krewer (2014) |
| $k_{II}$ | 0.25 | $dm^3\ s^{-1}$ | Daniel Schröder and Ulrike Krewer (2014) |
| $k_{III}^a$ | $2.37\times10^{-11}$ | $mol\ s^{-1}$ | Daniel Schröder and Ulrike Krewer (2014) |
| $k_{III}^c$ | $2.07\times10^{-11}$ | $mol\ s^{-1}$ | Daniel Schröder and Ulrike Krewer (2014) |
| $k_{H_2}^{electrolyte}$ | $1.29\times10^{-13}$ | $mol\ cm^{-3}s^{-1}$ | Deiss, Holzer et al. (2002) |

**Table A.2** Initial value for the presented simulation

| parameter | Value | unit |
|---|---|---|
| $c_{Zn(OH)_4^{2-}}^{zinc}$ | 0.66 | $mol\ dm^{-3}$ |
| $c_{Zn(OH)_4^{2-}}^{air}$ | 0.66 | $mol\ dm^{-3}$ |
| $c_{K^+}^{zinc}$ | 6.00 | $mol\ dm^{-3}$ |
| $c_{K^+}^{air}$ | 6.00 | $mol\ dm^{-3}$ |
| $c_{OH^-}^{zinc}$ | 4.68 | $mol\ dm^{-3}$ |
| $c_{OH^-}^{air}$ | 4.68 | $mol\ dm^{-3}$ |
| $c_{H_2O}^{zinc}$ | 50.35 | $mol\ dm^{-3}$ |
| $c_{H_2O}^{air}$ | 50.35 | $mol\ dm^{-3}$ |
| $c_{O_2}$ | $2.70\times10^{-5}$ (Tromans 1998) | $mol\ dm^{-3}$ |
| $c_{H_2}$ | 0.11 (Riietschi 1967) | $mol\ dm^{-3}$ |
| $\eta^{zinc}$ | 0 | $V$ |
| $\eta^{air}$ | 0 | $V$ |
| $V_{electrolyte}^{air}$ | $6.63\times10^{-5}$ | $dm^3$ |
| $V_{solid}^{zinc}$ | $n_{Zn}\cdot\tilde{V}_{Zn}+n_{ZnO}\cdot\tilde{V}_{ZnO}$ | $dm^3$ |
| $V_{electrolyte}^{zinc}$ | $1.5\cdot V_{solid}^{zinc}$ | $dm^3$ |
| $\delta_{electrode}^{zinc}$ | $\frac{V_{electrolyte}^{zinc}+V_{solid}^{zinc}}{A_{electrode}^{zinc}}$ | $dm$ |
| $n_{Zn}$ | $7.64\times10^{-4}$ | $mol$ |
| $n_{ZnO}$ | $5.50\times10^{-3}$ | $mol$ |

# VITA

Mr. Wacharaisuth Thanapong-amorn was born on April 25, 1992 in Chonburi province, Thailand. In 2010, he finished secondary school from Chonradsadornumrung School, Chonburi, Thailand. After that, he graduated the Bachelor's Degree in Chemical engineering from Kasetsart University of in 2014. He continued studying the Master's Degree of engineering in Chemical Engineering at Chulalongkorn University and joined Computational Process Engineering Research Center.